Published in final edited form as:
FEBS J. 2010 April ; 277(8): 1906–1920. doi:10.1111/j.1742-4658.2010.07613.x.

Anaerobic Sulfatase-Maturating Enzyme: A Mechanistic Link with Glycyl Radical Activating Enzymes?

Alhosna Benjdia[‡], **Sowmya Subramanian**[†], **Jérôme Leprince**[§], **Hubert Vaudry**[§], **Michael K. Johnson**[†], and **Olivier Berteau**[‡,*]

[‡] INRA, UMR1319 MICALIS, Domaine de Vilvert, F-78352 Jouy-en-Josas, France

[§] INSERM U413, IFRMP23, UA CNRS, Université de Rouen, 76821 Mont-Saint-Aignan, France

[†] Department of Chemistry and Center for Metalloenzyme Studies, University of Georgia, Athens, Georgia 30602, USA

Abstract

Sulfatases form a major group of enzymes present in prokaryotes and eukaryotes. This class of hydrolases is unique in requiring an essential post-translational modification of a critical active-site cysteinyl or seryl residue to C_α-formylglycine (FGly). Herein, we report mechanistic investigations of a unique class of radical-AdoMet enzymes, anSMEs (anaerobic sulfatase-maturating enzymes) which catalyze the oxidation of Cys-type and Ser-type sulfatases and possess three $[4Fe\text{-}4S]^{2+,+}$ clusters. We were able to develop a reliable quantitative enzymatic assay which allowed the direct measurement of FGly production and AdoMet cleavage. The results demonstrate stoichiometric coupling of AdoMet cleavage and FGly formation using peptide substrates with cysteinyl or seryl active-site residues. Analytical and EPR studies of the reconstituted wild-type enzyme and cysteinyl cluster mutants indicate the presence of three almost isopotential $[4Fe\text{-}4S]^{2+,+}$ clusters, each of which is required for *in vitro* FGly generation. More surprisingly, our data indicate that the two additional $[4Fe\text{-}4S]^{2+,+}$ clusters are required to obtain efficient reductive cleavage of AdoMet suggesting their involvement in the reduction of the radical AdoMet $[4Fe\text{-}4S]^{2+,+}$ center. These results, in addition to the recent demonstration of direct abstraction by anSMEs of the C_β H-atom from the active site cysteinyl or seryl residue using a 5′-deoxyadenosyl radical, provide new insights into the mechanism of this new class of radical-AdoMet enzymes.

Keywords

Sulfatase; Radical AdoMet Enzyme; Radical SAM enzyme; Iron sulfur center; S-adenosyl-L-methionine

Sulfatases belong to at least three mechanistically distinct groups, namely the Fe(II) α-ketoglutarate-dependent dioxygenases [1], the recently identified group of Zn-dependent alkylsulfatase [2] and the broad family of arylsulfatases [3]. This latter family of enzymes, termed “sulfatases” in this article, is certainly the most widespread among bacteria with some of them possessing more than one hundred sulfatase genes in their genomes [4]. Nevertheless, their biological function has almost never been investigated despite reports on their potential involvement in pathogenic processes [5,6].

Address correspondence to: Olivier Berteau at: INRA, UMR1319 MICALIS, Bât 440, Domaine de Vilvert, F-78352 Jouy-en-Josas, France. Olivier.Berteau@jouy.inra.fr.

Among hydrolases, sulfatases are unique in requiring an essential catalytic residue, a 3-oxoalanine usually called C_α-formylglycine (FGly) [7]. In sulfatases, it has been proposed that this modified amino acid is hydrated as a geminal diol in order to perform a nucleophilic attack on the sulfur atom of the substrate. This leads to the release of the desulfated product and the formation of a covalent sulfate-enzyme intermediate. The second hydroxyl group on the gem-diol is essential for the release of the inorganic sulfate as demonstrated by the inactivation of sulfatase bearing a seryl residue instead of the FGly residue [8].

This essential FGly residue results from the post-translational modification of a critical active-site cysteinyl or seryl residue (Fig. 1A). This has led to the classification of sulfatases into two sub-types, i.e. Cys-type and Ser-type sulfatases. In eukaryotes, only Cys-type sulfatases have been identified so far, while in bacteria, both types of sulfatases exist. Nevertheless, eukaryotic and prokaryotic sulfatases undergo identical post-translational modification involving the oxidation of a critical cysteinyl or a seryl residue into 3-oxoalanine.

In prokaryotes, 3-oxoalanine formation is catalyzed by at least three enzymatic systems but to date only two have been identified [9]. The first one, termed formylglycine-generating enzyme (FGE), uses molecular oxygen and an unidentified reducing agent in order to catalyze the aerobic conversion of the cysteinyl residue into FGly [10]. The second one, termed anaerobic sulfatase maturating enzyme (anSME), is a member of the *S*-adenosyl-L-methionine (AdoMet)-dependent superfamily of radical enzymes [11–13].

We have recently demonstrated that anSMEs are dual substrate enzymes able to catalyze the oxidation of cysteinyl or seryl residues making these enzymes responsible for the activation of both types sulfatase under anaerobic conditions [12]. Nevertheless, the mechanism by which these enzymes catalyze the anaerobic oxidation of cysteinyl or seryl residues is still obscure. Furthermore, in addition to the Cx_3Cx_2C motif that binds the $[4Fe\text{-}4S]^{2+,+}$ cluster common to all radical AdoMet superfamily enzymes, anSMEs have two additional conserved cysteinyl clusters with unknown functions.

In the present study, we have carried out mutagenesis studies to investigate the involvement of the conserved cysteinyl clusters in the anSME mechanism. Our data demonstrate that the additional conserved cysteinyl clusters bind two additional $[4Fe\text{-}4S]^{2+,+}$ centers which are required for FGly generation and efficient reductive cleavage of AdoMet suggesting that one or both of the additional $[4Fe\text{-}4S]^{2+,+}$ play a role in mediating the reduction of the radical-AdoMet $[4Fe\text{-}4S]^{2+,+}$ cluster.

RESULTS

Formylglycine and 5′-deoxyadenosine kinetics

The first step of the reaction catalyzed by all radical AdoMet enzymes investigated thus far is the reductive cleavage of AdoMet, *via* one-electron transfer from the enzyme $[4Fe\text{-}4S]^{+}$ center to AdoMet, to yield methionine and a 5′-deoxyadenosyl radical [14,15]. AdoMet is generally used as an oxidizing substrate with the noticeable exception of enzymes such as lysine 2,3-aminomutase [15,16] and spore photoproduct lyase [17–20] which use AdoMet catalytically. In other radical AdoMet enzymes, AdoMet is a co-substrate and as such one equivalent of AdoMet is used to oxidize one molecule of substrate. The only known exceptions are coproporphyrinogen III oxidase (HemN) which uses two AdoMet molecules per turnover for the decarboxylation of two propioniate side chains [21,22] and the radical AdoMet enzymes which catalyze sulfur insertion such as lipoyl synthase, biotin synthase and MiaB [14,15].

Recently Grove *et al.* characterized the *K. pneumoniae* anSME (anSMEkp) and investigated the maturation of a 18mer peptide, derived from the *K. pneumoniae* sulfatase sequence, containing the seryl residue target of the modification [23]. Quantitative data were extracted from HPLC and MALDI-TOF mass spectrometry analysis of the products. With the 18mer peptide substrate, three uncharacterized products and 5′-deoxyadenosine were observed by HPLC analysis and two peptide products were identified by mass spectrometry analysis. The expected FGly product (*i.e.* a 2-Da mass decrease, see Fig. 1A) was found to be a minor product in the mass spectrometry analysis, while the major product exhibited a 20-Da mass decrease and was tentatively attributed to the loss of a water molecule from the FGly product as a result of formation of a Schiff base *via* interaction between the aldehyde carbonyl of FGly and the N-terminal amino group. The three products observed in the HPLC analysis were not further characterized and it is not currently possible to state whether or not they are FGly-containing peptides, side reaction products or reaction intermediates. Nevertheless, based on the assumption that all three products observed by HPLC corresponded to or were derived from the FGly product, the authors concluded that anSMEs use one mole of AdoMet to produce one mole of FGly-containing peptide. While this is the most likely scenario based on mechanistic studies of other radical AdoMet enzymes, this result must be viewed as preliminary in light of the undetermined nature of the multiple peptide products.

Intrigued by the possibility that some of the peptides produced could be reaction intermediates, we have performed similar experiments with the *C. perfringens* enzyme (anSMEcpe) that was recently characterized in our laboratory [11,12]. In our previous studies, we used 23mer peptides as substrates [11,12]. Although these substrates proved to be satisfactory to demonstrate that anSMEs are able to catalyze the anaerobic oxidation of cysteinyl or seryl residues, the instability of these peptides prevented accurate quantifications of the enzymatic reaction. We thus investigated several peptides in order to find a more stable substrate and finally chose a 17mer peptide closer in size to the 18mer substrates used by Grove *et al* [23]. The substrate peptides used were Ac-TAVPS**C**IPSRASILTGM-NH_2 (**17C** peptide) ($[M+H]^+$ = 1745) and Ac-TAVPS**S**IPSRASILTGM-NH_2 (**17S** peptide) ($[M+H]^+$ = 1729). Upon incubation with anSMEcpe, both peptides were converted into a new species with a mass $[M+H]^+$ of 1727 Da (Fig. 1B, 1C & Fig. S1). This molecular mass was precisely the one expected for the conversion of the cysteinyl or the seryl residue into FGly. To further ascertain the nature of the modification, labeling experiments with 2,4-dinitrophenyl-hydrazine (DNPH) were performed [24]. A hydrazone derivative with a mass increment of 180 Da was formed demonstrating the presence of an aldehyde functional group in the newly formed peptide (supplementary data Fig. S2). Thus, in our experiments, only the substrate and the expected product were evident in the mass spectra and no other species appeared even after extended incubation (*i.e.* 12 hours with peptide 17S) (Fig. 1& Fig. S1&S2).

We then developed an HPLC-based assay that could provide reliable and direct quantitative data regarding the anSME activity. During incubation with each peptide, one new peptide appeared with a retention time of 20.4 min (Fig. 2A&B). The purification of this product and its MALDI-TOF MS analysis confirmed the nature of the product formed and kinetic experiments demonstrated that in both cases (*i.e.* with a cysteinyl or seryl containing peptide) a strict 1:1 coupling between AdoMet cleavage and FGly production occurred (Fig. 2C&D). AnSMEcpe exhibited a specific activity of 0.07 $nmol.min^{-1}.mg^{-1}$ with the 17S substrate, while the specific activity increased more than 15-fold (1.09 $nmol.min^{-1}.mg^{-1}$) for the 17C substrate.

Peptide 17A was initially included as a control to demonstrate that FGly production occurred on the target cysteinyl or seryl residue. As expected, in presence of enzyme, no

modification of the peptide 17A occurred (Fig. 2&S1C). Interestingly, AdoMet cleavage analysis in presence of this peptide showed that no 5′-dA was produced (Fig. 2D). This result is surprising because we previously showed that anSMEcpe alone, is able, under reducing conditions using sodium dithionite as electron donor, to produce 5′-dA from AdoMet [11]. This result suggests that non-productive peptides such as 17A bind near the active site and prevent either direct reduction of the $[4Fe\text{-}4S]^{2+,+}$ center or interaction with new AdoMet molecules.

Analytical and spectroscopic evidence for multiple Fe-S clusters in anSME— We previously demonstrated that anSMEs possess a typical radical AdoMet $[4Fe\text{-}4S]^{2+,+}$ center likely coordinated, as in all radical AdoMet enzymes, by the Cx_3Cx_2C motif [12]. Interestingly, in addition to this first conserved cysteine motif, anSMEs have 7 other strictly conserved cysteinyl residues and an additional cysteinyl residue in the C-terminus part of the protein (Fig. 3A). We and other groups [11,12,25,26] have proposed that additional iron-sulfur cluster(s) may be coordinated by the remaining conserved cysteinyl residues. Nevertheless, in our previous analytical and spectroscopic studies of as purified and reconstituted samples of WT anSMEcpe, we did not succeed in obtaining definitive evidence to support this proposal [11,12]. To address this issue, we used the *Bacteroides thetaiotaomicron* enzyme which proved to be more stable and produced three mutants in which groups of conserved cysteinyl residues were mutated to alanyl residues. The following mutants were generated: C24A/C28A/C31A variant (named mutant M_1), C276A/C282A (named mutant M_2) and C339A/C342A/C348A (named mutant M_3). Mutants were purified as previously described starting from a 15 L culture [12]. Purification of the mutants M_1 and M_2 proved to be satisfactory while mutant M_3 exhibited a major contamination which probably occurred from proteolytic cleavage (Fig. S3). All purified enzymes exhibited the typical brownish color of $[4Fe\text{-}4S]^{2+}$ cluster-containing enzymes and a broad shoulder centered near 400 nm (Fig. 3B).

The Fe-S cluster content of as-purified and reconstituted samples of WT and M_1 mutant anSMEbt were assessed by iron and protein analysis coupled with UV-visible absorption studies of oxidized and dithionite-reduced samples (Fig. S4) and EPR studies of dithionite reduced samples in the absence or presence of AdoMet (Fig. 4). As prepared samples of WT and M_1 mutant anSMEbt contained 6.3 ± 0.5 and 4.3 ± 0.5 Fe/monomer, respectively, that increased to 12.0 ± 1.0 and 10.8 ± 1.0 Fe/monomer, respectively, in reconstituted samples. In all cases the absorption spectra were characteristic of $[4Fe\text{-}4S]^{2+}$ clusters, i.e. broad shoulders centered at ~ 320 and ~ 400 nm. Moreover, the extinction coefficients at 400 nm mirror the Fe determinations and indicate 1.6 ± 0.2 and 1.1 ± 0.2 $[4Fe\text{-}4S]^{2+}$ clusters per monomer for the as-purified WT and M_1 mutant samples, respectively, and 2.8 ± 0.4 and 2.6 ± 0.4 $[4Fe\text{-}4S]^{2+}$ clusters per monomer for the reconstituted WT and M_1 mutant samples, respectively, based on the published range observed for single $[4Fe\text{-}4S]^{2+}$ clusters (ε_{400} = 14–18 $mM^{-1}cm^{-1}$) [27]. The $[4Fe\text{-}4S]^{2+}$ cluster content is likely to be an overestimate for the reconstituted M_1 mutant sample due to the increased absorption in the 600 nm region which generally indicates a contribution from adventitiously bound polymeric Fe-S species. While more quantitative analyses will require Mössbauer studies, the analytical and absorption data are consistent with WT and M_1 mutant anSMEbt being able to accommodate up to three and two $[4Fe\text{-}4S]^{2+}$ clusters per monomer, respectively. Hence the additional 7 or 8 conserved cysteinyl residues (see Fig. 3A) have the ability to coordinate two additional clusters. A similar conclusion was recently published for the homologous *Klebsiella pneumoniae* AtsB protein based on definitive analytical and Mössbauer studies [23].

Based on the absorption decrease at 400 nm on reduction, compared to well characterized $[4Fe\text{-}4S]^{2+,+}$ clusters, we estimate that ~20% and ~30% of the [4Fe-4S] clusters are reduced by dithionite in the reconstituted WT and M_1 mutant forms of anSMEbt, respectively**,** see

Fig. S4. Both samples exhibited weak, fast-relaxing EPR signals in the $S = 1/2$ region accounting for 0.12 spins/monomer for WT and 0.07 spins per monomer for the M_1 mutant (Fig. 4). The relaxation behavior (observable without relaxation broadening only below 30 K) is characteristic of $[4Fe\text{-}4S]^+$ clusters rather than $[2Fe\text{-}2S]^+$ clusters. The origin of the low spin $S = 1/2$ quantitations for dithionite-reduced WT and M_1 mutant anSMEbt, relative to the extent of reduction estimated based on absorption studies, is unclear at present. Most likely it is a consequence of $[4Fe\text{-}4S]^+$ clusters with $S = 1/2$ and 3/2 spin state heterogeneity as dithionite-reduced reconstituted samples of WT anSMEcpe with sub-stoichiometric cluster content (~6 Fe/monomer) exhibit weak features in the $g = 4–6$ region indicative of the low field components of the broad resonances spanning ~400 mT that are associated with $S = 3/2$ $[4Fe\text{-}4S]^+$ clusters [12]. As shown in Fig. S5, WT anSMEcpe exhibits well-resolved low-field $S = 3/2$ resonances in the $g = 4–6$ region that are perturbed in the presence of AdoMet suggesting that radical-AdoMet $[4Fe\text{-}4S]^+$ cluster contributes at least in part to the $S = 3/2$ EPR signal. In contrast, the fully reconstituted WT and M_1 mutant anSMEbt samples do not exhibit well-resolved resonances in the $g = 4–6$ region (data not shown). However, as indicated below, the lack of clearly observable $S = 3/2$ $[4Fe\text{-}4S]^+$ cluster resonances may well be a consequence of broadening due to intercluster spin-spin interaction involving the strongly paramagnetic $S = 3/2$ clusters in cluster replete samples of reduced anSMEbt.

The $S = 1/2$ resonance for the reduced M_1 mutant cannot be simulated as a single species and arises either from two distinct magnetically isolated $[4Fe\text{-}4S]^+$ clusters with approximately axial g tensors or as a result of weak magnetic interaction between two $[4Fe\text{-}4S]^+$ clusters. We suspect the latter, as two $S = 1/2$ resonances with different relaxation properties cannot be resolved based on temperature- and power-dependence studies. Such magnetic interactions would be expected to be greatly enhanced for clusters with $S = 3/2$ ground states resulting in additional broadening that would render the resonances unobservable except at inaccessibly high enzyme concentrations. However, irrespective of the explanation of the origin for the complex EPR signal exhibited by the dithionite-reduced M_1 mutant anSMEbt, the EPR data support the presence of two $[4Fe\text{-}4S]^{2+,+}$ clusters in addition to the radical-AdoMet $[4Fe\text{-}4S]^{2+,+}$ cluster in anSMEbt. Moreover, subtraction of the reduced M_1-mutant EPR spectrum from the reduced WT spectrum affords an axial resonance, $g_{||} = 2.04$ and $g_{\perp} = 1.92$, that is readily simulated as a magnetically isolated $S = 1/2$ $[4Fe\text{-}4S]^+$ cluster (accounting for 0.05 spins/monomer) and is attributed to the reduced radical-AdoMet $[4Fe\text{-}4S]^+$ cluster. This is confirmed by changes in the g values ($g = 1.98$, 1.90, 1.84) and increased spin quantitation (0.05 to 0.15 spins/monomer) for the $S = 1/2$ form of the radical-AdoMet $[4Fe\text{-}4S]^+$ cluster on addition of excess AdoMet (Fig. 4B). Similar changes in the EPR properties of radical-AdoMet $S = 1/2$ $[4Fe\text{-}4S]^+$ clusters on binding AdoMet have been reported for many radical-AdoMet enzymes [28,29] and the increase in spin quantitation is likely to be a consequence of the increase in redox potential that results from AdoMet binding [30]. In contrast, within the limits of experimental error, the EPR spectra and spin quantitation of the two additional $S = 1/2$ $[4Fe\text{-}4S]^+$ clusters that are present in the reduced M_1 mutant are not significantly perturbed by AdoMet.

Overall, the EPR and absorption results are best interpreted in terms of three $[4Fe\text{-}4S]^{2+,+}$ clusters in anSMEbt. Each is likely to be mixed spin ($S = 1/2$ and $S = 3/2$) in the reduced state and only one is capable of binding AdoMet at the unique Fe site. Since each is only partially reduced by dithionite at pH 7.5, their midpoint potentials are all likely to be in the range −400 to −450 mV.

Function of anSMEs cysteinyl clusters—Dierks and co-workers carried out pioneering studies to assess the function of the anSMEs cysteinyl clusters [25]. They made single amino acid variants in the three conserved cysteinyl clusters of anSMEkp and co-

expressed these mutants in *E. coli*, along with the sulfatase from *K. pneumonia*. All mutants failed to mature the co-expressed sulfatase as no sulfatase activity could be measured. Nevertheless, it was not possible to conclude whether the mutated enzymes were unable to catalyze any reaction or led to the formation of reaction intermediates like spore photoproduct lyase (SPL), another radical AdoMet enzyme, for which it has been elegantly demonstrated that a cysteinyl mutant, while inactive *in vivo* [31], efficiently catalyzes *in vitro* AdoMet cleavage with substrate H-atom abstraction leading to the formation of a side product [18].

We thus assayed the *in vitro* activity of anSMEbt wild type and mutants after reconstitution in presence of iron and sulfide. All proteins exhibited UV-visible spectra compatible with the presence of [4Fe-4S] centers (Fig. 3B). Enzymatic assays were conducted using 17C peptide as a substrate and reactions were analyzed by HPLC and MALDI-TOF MS. The results demonstrate that WT anSMEbt is able to mature the substrate peptide, but that none of the mutant forms, *i.e.* M_1, M_2, or M_3, were able to catalyze peptide maturation or to produce a peptidyl intermediate, as no other peptide was observed by HPLC or MALDI-TOF MS analysis (Fig. 5A&B). Even after derivatization with DNPH, which strongly enhances the signal of the FGly-containing peptide, no trace of modified peptide could be detected using the M_1, M_2, or M_3 mutants (Fig. S6).

AdoMet cleavage was assessed for WT and M_1, M_2, or M_3 variants of anSMEbt using the HPLC assay. As expected, the results showed that mutant M_1, which lacks the radical AdoMet cysteinyl cluster, is unable to produce 5′-dA contrary to the wild type enzyme (Fig. 5C). More surprisingly, HPLC analyses revealed that the reductive cleavage of AdoMet was also strongly inhibited in the M_2 and M_3 mutants with a 50 to 100-fold decrease compared to the WT enzyme (Fig. 5D).

The variant proteins were also incubated with AdoMet under reducing conditions in the absence of substrate, as we previously reported that anSMEbt is able to produce 5′-dA efficiently under these conditions [12]. In the absence of substrate, the AdoMet reductive cleavage activity of all mutants was identical to the one obtained in presence of peptide again indicating that all three clusters are required for effective reductive cleavage of AdoMet. This observation is most readily interpreted in terms of a role for the two additional $[4Fe\text{-}4S]^{2+,+}$ clusters in mediating electron transfer to the radical-AdoMet $[4Fe\text{-}4S]^{2+,+}$ cluster. A similar interpretation was made to explain the strong inhibition of AdoMet reductive cleavage that was observed in the 4-hydroxyphenylacetate decarboxylase activating enzyme, a radical AdoMet enzyme possessing three [4Fe-4S] centers, when cysteinyl residues in its two additional cysteinyl clusters were mutated to alanines [32]. However, in the absence of detailed spectroscopic characterization of the clusters in the M_2 and M_3 mutant anSMEbt samples, we cannot rule out the possibility that the loss of one of the additional [4Fe-4S] clusters affects the ability to reductively cleave AdoMet by perturbing the redox potential, AdoMet-binding ability or assembly of the radical-AdoMet $[4Fe\text{-}4S]^{2+,+}$ cluster.

Sequences comparison with other radical AdoMet enzymes—Primary sequence comparisons with previously studied radical AdoMet enzymes did not reveal significant homologies, but several other radical AdoMet enzymes catalyzing post-translational protein modifications contain conserved cysteinyl clusters involved in the coordination of additional [4Fe-4S] centers. These enzymes are B_{12}-independent glycyl radical activating enzymes (GRE-AE), *i.e.* benzylsuccinate synthase [33], glycerol dehydratase [34,35] and 4-hydroxyphenylacetate decarboxylase [32] activases, which catalyze the formation of a glycyl radical on their respective cognate enzyme using 5′-deoxyadenosyl radical. The role of these additional clusters has still to be established, but preliminary mutagenesis studies

for a hydroxyphenylacetate decarboxylase activating enzyme indicated a role in mediating electron transfer to the radical-AdoMet [4Fe-4S] cluster [32].

Further examination of radical AdoMet enzymes involved in protein or peptide modification lead to the identification of several proteins sharing the third cysteinyl cluster, $Cx_2Cx_5Cx_3C$, located in their C-terminal parts while the second cysteinyl cluster found in anSME could only be tentatively assigned in the central part of these proteins (Fig. 6). These proteins are the activating enzyme involved in quinohemoprotein amine dehydrogenase biosynthesis (QHNDH-AE) which is involved in the cross-linking of cysteinyl residues with glutamate and aspartate residue [36] and a new radical AdoMet enzyme involved in the biosynthesis of a cyclic peptide through a lysine-tryptophan linkage (ST protein) [37]. Although not strictly conserved, we also identified this cluster in PqqE, an enzyme involved in pyrroloquinoline quinone biosynthesis and proposed to catalyze the linkage of glutamate and tyrosine moieties [38]. All these proteins, despite not being homologous, have conserved cysteinyl clusters and catalyze various amino acid modifications. It is thus likely that all these enzymes share common features with anSMEs and notably the presence of additional [4Fe-4S] centers as demonstrated for PqqE [39].

DISCUSSION

We recently demonstrated that sulfatase maturation catalyzed by the radical AdoMet enzyme anSME is initiated by C_βH-atom abstraction [40]. Nevertheless, the entire mechanism of this enzyme has not yet been deciphered. The results presented herein using a new anSME substrate facilitate more definitive conclusions concerning the catalytic mechanism of anSME and the AdoMet requirement. Indeed, using a HPLC-based quantitative assay, we have demonstrated tight 1:1 coupling between AdoMet cleavage and FGly production using both cysteinyl- and seryl- containing peptides. We also demonstrate tight inhibition of AdoMet reductive cleavage when the target residue is substituted by an alanyl residue contrary to what happens in absence of the substrate. Our interpretation is that the peptide binding at the enzyme active site prevents AdoMet access to the active site. The recently solved crystal structure of another radical AdoMet enzyme, PFL-AE [41], has demonstrated that such a hypothesis is structurally valid. In PFL-AE, the [4Fe-4S] cluster and AdoMet are deeply buried, thereby preventing uncoupling between AdoMet cleavage and glycyl radical generation.

A longstanding question about anSMEs concerns the function of the conserved additional cysteinyl clusters originally identified by Schrimer and Kolter [26]. In this bioinformatics study, it was suggested that these clusters were involved in [Fe-S] center coordination. The mutagenesis of these conserved residues in the *K. pneumoniae* enzyme subsequently revealed that they are essential for *in vivo* activity [25]. Nevertheless, their function remained elusive. Grove *et al.* provided the first definitive evidence that they are involved with coordinating two [4Fe-4S] centers in addition to the radical AdoMet [4Fe-4S] center [23]. Based on the inferred AdoMet requirement, a mechanism was proposed involving site-specific ligation of one of the additional $[4Fe\text{-}4S]^{2+}$ centers to the target cysteinyl or seryl residue resulting in substrate deprotonation. The 5′-deoxyadenosyl radical generated by reductive cleavage of AdoMet bound at the unique site of radical AdoMet $[4Fe\text{-}4S]^{2+,+}$ cluster would then abstract a C_β hydrogen atom from the target residue and an aldehyde product is generated by using the cluster as the conduit for removal of the second electron [23]. The proposed mechanism is reminiscent of the isopenicillin N synthase (IPNS) which catalyzes the C_β-H cleavage from a cysteinyl residue after its coordination by a mononuclear non-heme iron center. Following H-atom abstraction, a postulated thioaldehyde intermediate is formed leading to peptide cyclization [42,43]. Interestingly, using substrate analogues it

has been reported that IPNS can oxidize its target cysteinyl residue into a hydrated aldehyde which is virtually the same as the reaction catalyzed by anSME [44].

Thus, it is conceivable that one of the two additional clusters binds and deprotonates the target cysteinyl or seryl residues and provides a conduit for removal of the second electron [23]. If such mechanism is correct, our recent demonstration that the 5′-deoxyadenosyl radical produced by anSME directly abstracts one of the cysteinyl C_β hydrogen atoms [40], coupled with the results reported herein, indicate that deprotonation occurs prior to or simultaneously with AdoMet cleavage. Indeed, using an alanyl containing peptide we observed complete inhibition of AdoMet cleavage.

Although the mutagenesis studies reported herein suggest that both of the two additional [4Fe-4S] clusters are required for AdoMet cleavage using dithionite as an electron donor, we cannot rule out the possibility that this is a consequence of perturbation of the redox or AdoMet-binding properties of the radical-AdoMet $[4Fe\text{-}4S]^{2+,+}$ center that are induced by loss of either the two additional clusters. Hence it is possible that one of the additional [4Fe-4S] clusters (Cluster II) is involved with binding the peptide substrate and providing a conduit for removal of the second electron. The other [4Fe-4S] cluster (Cluster III) could function in mediating electron transfer from the physiological electron donor to the radical-AdoMet [4Fe-4S] cluster or from Cluster II to the physiological electron acceptor, see Fig. 7A. The former mechanism is analogous to that recently proposed by Grove et al [23].

Nevertheless, the data presented herein suggests an alternative mechanism. Indeed, the primary sequence analyses discussed above indicate that the two additional clusters are likely to be ligated by the 8 conserved cysteinyl residues and hence both [4Fe-4S] clusters may have complete cysteinyl ligation, one cysteinyl residue from the last motif being involved in the coordination of the second cluster (Fig. 3A). Furthermore, the preliminary observation that these clusters are almost isopotential with the radical-AdoMet cluster and the mutagenesis studies reported herein which indicate that both additional [4Fe-4S] clusters are required for productive reductive cleavage of AdoMet, both suggest that the additional $[4Fe\text{-}4S]^{2+,+}$ clusters play a role in facilitating electron transfer to the radical-AdoMet cluster, as appears to be the case in some GRE-AEs [32]. Finally, sequence analysis revealed that these cysteinyl clusters are also found in other radical AdoMet enzymes involved in protein or peptide modification. These enzymes catalyze the modification of amino acids such as glutamate or tyrosine which are not known to bind [Fe-S] centers. Moreover, another radical AdoMet enzyme, BtrN, has recently been demonstrated to use AdoMet stoichiometrically to catalyze the two electron oxidation of a hydroxyl group to a ketone without additional Fe-S centers, a reaction formally analogous to the one catalyzed by anSME [45]. However, the absence of additional Fe-S clusters in BtrN clearly requires confirmation using Mössbauer spectroscopy.

Based on the above considerations, we propose an alternate mechanism for anSME (Fig. 7B). In our proposed mechanism, the initial step is the reduction of the radical-AdoMet $[4Fe\text{-}4S]^{2+}$ cluster *via* electron transfer from the two additional $[4Fe\text{-}4S]^{2+,+}$ clusters. Following this reduction, the C_βH-atom of the substrate is abstracted by the 5′-deoxyadenosyl radical generated by the reductive cleavage of AdoMet bound at the radical-AdoMet $[4Fe\text{-}4S]^{2+,+}$ cluster as recently demonstrated [40]. Simultaneously, deprotonation of the thiol or hydroxyl group occurs catalyzed by an amino acid side chain. The substrate radical intermediate formed by C_βH-atom abstraction is then further oxidized to yield an aldehyde or a thioaldehyde. In this scenario, the radical would be transferred back to the radical-AdoMet $[4Fe\text{-}4S]^{2+}$ cluster by outer-sphere electron transfer. The implication is that the reaction would have a substrate radical intermediate, as recently demonstrated for BtrN [45], and would be self-sustaining once the initial electron has been supplied by an

exogenous electron donor. Both possibilities are currently under investigation in our laboratories.

For Cys-type sulfatases, both mechanisms shown in Fig. 7 result in the formation of a thioaldehyde intermediate as is also the case in IPNS [42] and cysteine decarboyxlases [46,47]. Hydrolysis of the thioaldehyde by a water molecule is the likely next step. In accord with this hypothesis ^{18}O incorporation into the FGly-residue is observed when the reaction is carried out in $H_2{}^{18}O$ buffer, see Fig. S7.

If more work needs to be done to clarify the catalytic mechanism of anSMEs and the role of the two additional [4Fe-4S] clusters, the present report suggests that anSMEs possess common features with some glycyl radical activating enzymes and that radical AdoMet enzymes possessing additional [4Fe-4S] clusters are likely to be found notably in enzymes catalyzing protein post-translational modifications. It remains to be seen if the function of these additional clusters involves mediating electron transfer and/or binding and activating the peptidyl substrates.

EXPERIMENTAL PROCEDURES

Chemicals

All chemicals and reagents were obtained from commercial sources and were of analytical grade. *S*,*S*-Adenosyl-L-methionine (AdoMet) was synthesized enzymatically and purified as described previously [17].

anSMEcpe and anSMEbt protein expression and purification

Protein expression and purification were performed as previously described [12]. Briefly, *E. coli* BL21 (DE3) transformed with a plasmid bearing the *anSMEcpe* or the *anSMEbt* gene (pET-6His-*anSMEcpe* or pET-6His-*anSMEbt*) were grown aerobically overnight at 37°C in LB medium (100 mL) supplemented with kanamycin (50 $\mu g.mL^{-1}$). An overnight culture was then used to inoculate fresh LB medium (15 L) supplemented with the same antibiotic. After overnight growth at 25°C in the presence of IPTG, cells were collected and suspended in Tris-buffer (50 mM Tris, 150 mM KCl, 10% glycerol pH 7.5). The cells were then disrupted by sonication and centrifuged at 220,000 ×g at 4°C for 1 hour. The solution was then loaded onto a Ni-NTA Sepharose column equilibrated with Tris-buffer, pH 7.5. The column was washed extensively with the same buffer. Some of the adsorbed proteins were eluted by a washing step with 25 and 100 mM imidazole and the over-expressed protein was eluted by applying 500 mM imidazole. Imidazole was removed by gel filtration chromatography PD-10 columns (GE Healthcare) and fractions containing the anSMEcpe or anSMEbt proteins were immediately concentrated using Ultrafree cells (Millipore) with a molecular cut-off of 10 kDa.

Construction of cysteinyl cluster mutants

AnSMEbt mutants were obtained using the QuikChange site-directed mutagenesis kit (Stratagene). For each mutant a two-step PCR method was used [48]. The following primers were used for C24A/C28A/C31A mutant: 5′-GCC GTA **GCC** AAC CTC GCA **GCC** GAA TAC **GCC** TAT TAT-3′ and 5′-ATA ATA **GGC** GTA TTC **GGC** TGC GAG GTT **GGC** TAC GGC-3′ for C276A/C282A mutant: 5′-GGC GTA **GCT** ACA ATG GCG AAG CAT **GCC** GGA CAT-3′ and 5′-ATG TCC **GGC** ATG CTT CGC CAT TGT **AGC** TAC GCC-3′ and for C339A/C342A/C348A mutant: 5′-ACC CAA **GCC** AAG GAG **GCC** GAC TTT CTA TTT GCC **GCC** AAC GGA-3′ and 5′-TCC GTT **GGC** GGC AAA TAG AAA GTC **GGC** CTC CTT **GGC** TTG GGT-3′ (in bold are indicated the changed codons). After verification of the correct mutation by sequencing, the plasmid obtained were transformed

into *E. coli* BL21 (DE3) and the mutated proteins produced using the same protocol as the wild-type enzyme.

Reconstitution of Fe-S clusters on anSMEbt and anSMEcpe

Reconstitution was carried out anaerobically in a glove box (Bactron IV). Anaerobically purified anSMEs (200 μM monomer) were treated with 5 mM DTT (SIGMA, St Louis, MO, USA) and incubated overnight with a 10-fold molar excess of both Na_2S (SIGMA, St Louis, MO, USA). and $(NH_4)_2Fe(SO_4)_2$ (SIGMA, St Louis, MO, USA) at 12°C. The proteinwas desalted using a Sephadex G25 column (GE Healthcare, WI, USA) and thecolored fractions were concentrated on Amicon Ultra-4 (Millipore, Billerica, MA, USA). Protein concentrations were determined by the Bradford protein assay (SIGMA, St Louis, MO, USA), using BSA as a standard. Iron concentrations were determined colorimetrically using bathophenanthroline (SIGMA, St Louis, MO, USA) under reducing conditions, after digestion of the protein in 0.8% $KMnO_4$/0.2 M HCl.

Peptide synthesis

The following 17-mer peptides (with the critical residue in bold): Ac-TAVPS**C**IPSRASILTGM-NH_2, Ac-TAVPS**S**IPSRASILTGM-NH_2 and Ac-TAVPS**A**IPSRASILTGM-NH_2 were synthesized (0.1-mmol scale) by the solid phase methodology on a Rink amide 4-methylbenzhydrylamine resin (VWR, Fontenay-sous-Bois, France) by using a 433A Applied Biosystems peptide synthesizer (Applera-France, Courtaboeuf, France) and the standard Fmoc manufacturer's procedure. The synthetic peptides were purified by reversed-phase HPLC on a 2.2 × 25-cm Vydac 218TP1022 C_{18} column (Alltech, Templemars, France) by using a linear gradient (10–50% over 45 min) of acetonitrile/trifluoroacetic acid (TFA) (99.9: 0.1; v/v) at a flow rate of 10 mL/min. Analytical HPLC, performed on a 0.46 × 25-cm Vydac 218TP54 C_{18} column (Alltech), showed that the purity of the peptides was >99.1%. The purified peptides were characterized by MALDI-TOF mass spectrometry on a Voyager DE PRO (Applera, France) in the reflector mode with α-cyano-4-hydroxycinnamic acid as a matrix.

Peptide maturation

Samples containing 6 mM dithiothreitol, 3 mM sodium dithionite, 500 μM peptides and 1 mM AdoMet in Tris-buffer, pH 7.5 were incubated with reconstituted proteins. The reactions were performed in an anaerobic glovebox (Bactron IV). The oxygen concentration was monitored with a gas analyzer (Coy Laboratory). After incubation at 25°C, samples were divided in half, one part was used to test the maturation activity by mass spectrometry while the other half was used to quantify the reductive cleavage of AdoMet and FGly formation. Control samples were prepared without enzyme to verify peptide and AdoMet stability over time. Experiments performed in $H_2{}^{18}O$ were made exactly as described above except that the Tris-buffer was made in $H_2{}^{18}O$ and the enzyme was exchanged twice with this buffer before the experiments.

Peptide maturation analysis by MALDI-TOF MS

The α-cyano-4-hydroxycinnamic acid matrix (CHCA) (SIGMA, St Louis, MO, USA) was prepared at 4 $mg.mL^{-1}$ in 0.15% TFA, 50% acetonitrile. The 2,4-dinitrophenylhydrazone acid matrix (DNPH) was prepared at 100 $mg.mL^{-1}$ in 0.15% TFA, 50% acetonitrile. Equal volumes (1 μL) of matrix and sample were spotted onto the MALDI-TOF target plate. MALDI-TOF analysis was then performed on a Voyager DE STR Instrument (Applied Biosystems, Framingham, CA). Spectra were acquired in the reflector mode with: 20 kV accelerating voltage, 62% grid voltage and a 120 ns delay.

Peptide maturation and 5′-deoxyadenosine production quantification by HPLC

Peptide modification and 5′-deoxyadenosine production was measured by high-performance liquid chromatography using a C_{18} column (LicroSphere, 5-μm, 4.6 × 150-mm) equilibrated in solvent A (0.1% trifluoroacetic acid). A linear gradient from 0 to 80% acetonitrile was applied at a constant flow rate of 1 mL/min. Detection was carried out at 260 nm for *S*-adenosylmethionine and its derivative and at 215 nm to follow peptide modification.

Electron paramagnetic resonance (EPR)

X-band EPR spectra were recorded on a Bruker Instruments ESP 300D spectrometer equipped with an Oxford Instruments ESR 900 flow cryostat (4.2–300 K). Spectra were quantified under non-saturating conditions by double integration against a 1 mM CuEDTA standard.

Supplementary Material

Refer to Web version on PubMed Central for supplementary material.

Acknowledgments

This work was supported by grants from Agence Nationale de la Recherche (Grant ANR-08-BLAN-0224-02) and the NIH to M.K.J. (GM62524). Mass spectrometry experiments were performed at PAPSSO, INRA, Jouy-en-Josas.

References

1. Muller I, Kahnert A, Pape T, Sheldrick GM, Meyer-Klaucke W, Dierks T, Kertesz M, Uson I. Crystal structure of the alkylsulfatase AtsK: insights into the catalytic mechanism of the Fe(II) alpha-ketoglutarate-dependent dioxygenase superfamily. Biochemistry. 2004; 43:3075–3088. [PubMed: 15023059]
2. Hagelueken G, Adams TM, Wiehlmann L, Widow U, Kolmar H, Tummler B, Heinz DW, Schubert WD. The crystal structure of SdsA1, an alkylsulfatase from Pseudomonas aeruginosa, defines a third class of sulfatases. Proc Natl Acad Sci U S A. 2006; 103:7631–7636. [PubMed: 16684886]
3. Hanson SR, Best MD, Wong CH. Sulfatases: structure, mechanism, biological activity, inhibition, and synthetic utility. Angew Chem Int Ed Engl. 2004; 43:5736–5763. [PubMed: 15493058]
4. Glockner FO, Kube M, Bauer M, Teeling H, Lombardot T, Ludwig W, Gade D, Beck A, Borzym K, Heitmann K, Rabus R, Schlesner H, Amann R, Reinhardt R. Complete genome sequence of the marine planctomycete Pirellula sp. strain 1. Proc Natl Acad Sci U S A. 2003; 100:8298–8303. [PubMed: 12835416]
5. Hoffman JA, Badger JL, Zhang Y, Huang SH, Kim KS. Escherichia coli K1 aslA contributes to invasion of brain microvascular endothelial cells in vitro and in vivo. Infect Immun. 2000; 68:5062–5067. [PubMed: 10948126]
6. Tralau T, Vuilleumier S, Thibault C, Campbell BJ, Hart CA, Kertesz MA. Transcriptomic analysis of the sulfate starvation response of Pseudomonas aeruginosa. J Bacteriol. 2007; 189:6743–6750. [PubMed: 17675390]
7. Schmidt B, Selmer T, Ingendoh A, von Figura K. A novel amino-acid modification in sulfatases that is defective in multiple sulfatase deficiency. Cell. 1995; 82:271–278. [PubMed: 7628016]
8. Recksiek M, Selmer T, Dierks T, Schmidt B, von Figura K. Sulfatases, trapping of the sulfated enzyme intermediate by substituting the active site formylglycine. J Biol Chem. 1998; 273:6096–6103. [PubMed: 9497327]
9. Benjdia A, Deho G, Rabot S, Berteau O. First evidences for a third sulfatase maturation system in prokaryotes from E. coli aslB and ydeM deletion mutants. FEBS Lett. 2007; 581:1009–1014. [PubMed: 17303125]
10. Carlson BL, Ballister ER, Skordalakes E, King DS, Breidenbach MA, Gilmore SA, Berger JM, Bertozzi CR. Function and structure of a prokaryotic formylglycine-generating enzyme. J Biol Chem. 2008; 283:20117–20125. [PubMed: 18390551]

11. Benjdia A, Leprince J, Guillot A, Vaudry H, Rabot S, Berteau O. Anaerobic sulfatase-maturating enzymes: radical SAM enzymes able to catalyze in vitro sulfatase post-translational modification. J Am Chem Soc. 2007; 129:3462–3463. [PubMed: 17335281]
12. Benjdia A, Subramanian S, Leprince J, Vaudry H, Johnson MK, Berteau O. Anaerobic sulfatase-maturating enzymes - first dual substrate radical S-adenosylmethionine enzymes. J Biol Chem. 2008; 283:17815–17826. [PubMed: 18408004]
13. Berteau O, Guillot A, Benjdia A, Rabot S. A new type of bacterial sulfatase reveals a novel maturation pathway in prokaryotes. J Biol Chem. 2006; 281:22464–22470. [PubMed: 16766528]
14. Fontecave M, Atta M, Mulliez E. S-adenosylmethionine: nothing goes to waste. Trends Biochem Sci. 2004; 29:243–249. [PubMed: 15130560]
15. Frey PA, Hegeman AD, Ruzicka FJ. The Radical SAM Superfamily. Crit Rev Biochem Mol Biol. 2008; 43:63–88. [PubMed: 18307109]
16. Chen D, Walsby C, Hoffman BM, Frey PA. Coordination and mechanism of reversible cleavage of S-adenosylmethionine by the [4Fe-4S] center in lysine 2,3-aminomutase. J Am Chem Soc. 2003; 125:11788–11789. [PubMed: 14505379]
17. Chandor A, Berteau O, Douki T, Gasparutto D, Sanakis Y, Ollagnier-de-Choudens S, Atta M, Fontecave M. Dinucleotide spore photoproduct, a minimal substrate of the DNA repair spore photoproduct lyase enzyme from Bacillus subtilis. J Biol Chem. 2006; 281:26922–26931. [PubMed: 16829676]
18. Chandor-Proust A, Berteau O, Douki T, Gasparutto D, Ollagnier-de-Choudens S, Fontecave M, Atta M. DNA repair and free radicals, new insights into the mechanism of spore photoproduct lyase revealed by single amino acid substitution. J Biol Chem. 2008; 283:36361–36368. [PubMed: 18957420]
19. Cheek J, Broderick JB. Direct H atom abstraction from spore photoproduct C-6 initiates DNA repair in the reaction catalyzed by spore photoproduct lyase: evidence for a reversibly generated adenosyl radical intermediate. J Am Chem Soc. 2002; 124:2860–2861. [PubMed: 11902862]
20. Friedel MG, Berteau O, Pieck JC, Atta M, Ollagnier-de-Choudens S, Fontecave M, Carell T. The spore photoproduct lyase repairs the 5S- and not the 5R-configured spore photoproduct DNA lesion. Chem Commun (Camb). 2006:445–447. [PubMed: 16493831]
21. Layer G, Kervio E, Morlock G, Heinz DW, Jahn D, Retey J, Schubert WD. Structural and functional comparison of HemN to other radical SAM enzymes. J Biol Chem. 2005; 386:971–980.
22. Layer G, Moser J, Heinz DW, Jahn D, Schubert WD. Crystal structure of coproporphyrinogen III oxidase reveals cofactor geometry of Radical SAM enzymes. EMBO J. 2003; 22:6214–6224. [PubMed: 14633981]
23. Grove TL, Lee KH, St Clair J, Krebs C, Booker SJ. In vitro characterization of AtsB, a radical SAM formylglycine-generating enzyme that contains three [4Fe-4S] clusters. Biochemistry. 2008; 47:7523–7538. [PubMed: 18558715]
24. Peng J, Schmidt B, von Figura K, Dierks T. Identification of formylglycine in sulfatases by matrix-assisted laser desorption/ionization time-of-flight mass spectrometry. J Mass Spectrom. 2003; 38:80–86. [PubMed: 12526009]
25. Fang Q, Peng J, Dierks T. Post-translational formylglycine modification of bacterial sulfatases by the radical S-adenosylmethionine protein AtsB. J Biol Chem. 2004; 279:14570–14578. [PubMed: 14749327]
26. Schirmer A, Kolter R. Computational analysis of bacterial sulfatases and their modifying enzymes. Chem Biol. 1998; 5:R181–186. [PubMed: 9710560]
27. Agar JN, Krebs C, Frazzon J, Huynh BH, Dean DR, Johnson MK. IscU as a scaffold for iron-sulfur cluster biosynthesis: sequential assembly of [2Fe-2S] and [4Fe-4S] clusters in IscU. Biochemistry. 2000; 39:7856–7862. [PubMed: 10891064]
28. Fontecave M. Iron-sulfur clusters: ever-expanding roles. Nat Chem Biol. 2006; 2:171–174. [PubMed: 16547473]
29. Wang SC, Frey PA. S-adenosylmethionine as an oxidant: the radical SAM superfamily. Trends Biochem Sci. 2007; 32:101–110. [PubMed: 17291766]

30. Wang SC, Frey PA. Binding energy in the one-electron reductive cleavage of S-adenosylmethionine in lysine 2,3-aminomutase, a radical SAM enzyme. Biochemistry. 2007; 46:12889–12895. [PubMed: 17944492]

31. Fajardo-Cavazos P, Rebeil R, Nicholson WL. Essential cysteine residues in Bacillus subtilis spore photoproduct lyase identified by alanine scanning mutagenesis. Curr Microbiol. 2005; 51:331–335. [PubMed: 16163454]

32. Yu L, Blaser M, Andrei PI, Pierik AJ, Selmer T. 4-Hydroxyphenylacetate decarboxylases: properties of a novel subclass of glycyl radical enzyme systems. Biochemistry. 2006; 45:9584–9592. [PubMed: 16878993]

33. Leuthner B, Leutwein C, Schulz H, Horth P, Haehnel W, Schiltz E, Schagger H, Heider J. Biochemical and genetic characterization of benzylsuccinate synthase from Thauera aromatica: a new glycyl radical enzyme catalysing the first step in anaerobic toluene metabolism. Mol Microbiol. 1998; 28:615–628. [PubMed: 9632263]

34. O'Brien JR, Raynaud C, Croux C, Girbal L, Soucaille P, Lanzilotta WN. Insight into the mechanism of the B12-independent glycerol dehydratase from Clostridium butyricum: preliminary biochemical and structural characterization. Biochemistry. 2004; 43:4635–4645. [PubMed: 15096031]

35. Raynaud C, Sarcabal P, Meynial-Salles I, Croux C, Soucaille P. Molecular characterization of the 1,3-propanediol (1,3-PD) operon of Clostridium butyricum. Proc Natl Acad Sci U S A. 2003; 100:5010–5015. [PubMed: 12704244]

36. Ono K, Okajima T, Tani M, Kuroda S, Sun D, Davidson VL, Tanizawa K. Involvement of a putative [Fe-S]-cluster-binding protein in the biogenesis of quinohemoprotein amine dehydrogenase. J Biol Chem. 2006; 281:13672–13684. [PubMed: 16546999]

37. Ibrahim M, Guillot A, Wessner F, Algaron F, Besset C, Courtin P, Gardan R, Monnet V. Control of the transcription of a short gene encoding a cyclic peptide in Streptococcus thermophilus: a new quorum-sensing system? J Bacteriol. 2007; 189:8844–8854. [PubMed: 17921293]

38. Puehringer S, Metlitzky M, Schwarzenbacher R. The pyrroloquinoline quinone biosynthesis pathway revisited: a structural approach. BMC Biochem. 2008; 9:8. [PubMed: 18371220]

39. Wecksler SR, Stoll S, Tran H, Magnusson OT, Wu SP, King D, Britt RD, Klinman JP. Pyrroloquinoline quinone biogenesis: demonstration that PqqE from Klebsiella pneumoniae is a radical S-adenosyl-L-methionine enzyme. Biochemistry. 2009; 48:10151–10161. [PubMed: 19746930]

40. Benjdia A, Leprince J, Sandstrom C, Vaudry H, Berteau O. Mechanistic investigations of anaerobic sulfatase-maturating enzyme: direct Cbeta H-atom abstraction catalyzed by a radical AdoMet enzyme. J Am Chem Soc. 2009; 131:8348–8349. [PubMed: 19489556]

41. Vey JL, Yang J, Li M, Broderick WE, Broderick JB, Drennan CL. Structural basis for glycyl radical formation by pyruvate formate-lyase activating enzyme. Proc Natl Acad Sci U S A. 2008; 105:16137–16141. [PubMed: 18852451]

42. Bollinger JM Jr, Krebs C. Enzymatic C-H activation by metal-superoxo intermediates. Curr Opin Chem Biol. 2007; 11:151–158. [PubMed: 17374503]

43. Burzlaff NI, Rutledge PJ, Clifton IJ, Hensgens CM, Pickford M, Adlington RM, Roach PL, Baldwin JE. The reaction cycle of isopenicillin N synthase observed by X-ray diffraction. Nature. 1999; 401:721–724. [PubMed: 10537113]

44. Long AJ, Clifton IJ, Roach PL, Baldwin JE, Rutledge PJ, Schofield CJ. Structural studies on the reaction of isopenicillin N synthase with the truncated substrate analogues delta-(L-alpha-aminoadipoyl)-L-cysteinyl-glycine and delta-(L-alpha-aminoadipoyl)-L-cysteinyl-D-alanine. Biochemistry. 2005; 44:6619–6628. [PubMed: 15850395]

45. Yokoyama K, Ohmori D, Kudo F, Eguchi T. Mechanistic study on the reaction of a radical SAM dehydrogenase BtrN by electron paramagnetic resonance spectroscopy. Biochemistry. 2008; 47:8950–8960. [PubMed: 18672902]

46. Strauss E, Zhai H, Brand LA, McLafferty FW, Begley TP. Mechanistic studies on phosphopantothenoylcysteine decarboxylase: trapping of an enethiolate intermediate with a mechanism-based inactivating agent. Biochemistry. 2004; 43:15520–15533. [PubMed: 15581364]

47. Blaesse M, Kupke T, Huber R, Steinbacher S. Crystal structure of the peptidyl-cysteine decarboxylase EpiD complexed with a pentapeptide substrate. EMBO J. 2000; 19:6299–6310. [PubMed: 11101502]

48. Wang W, Malcolm BA. Two-stage PCR protocol allowing introduction of multiple mutations, deletions and insertions using QuikChange Site-Directed Mutagenesis. Biotechniques. 1999; 26:680–682. [PubMed: 10343905]

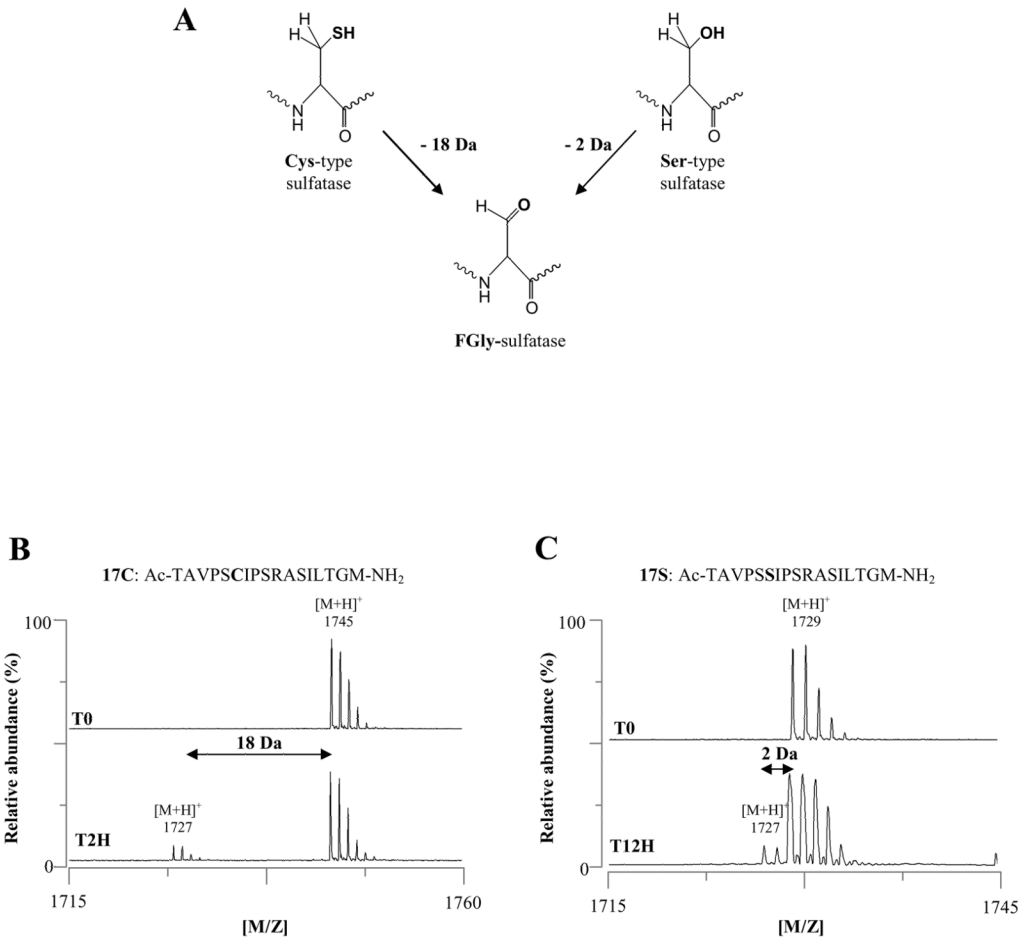

Figure 1. Sulfatase maturation scheme leading from a cysteinyl or seryl residue to a C_α-formylglycine residue (FGly) in sulfatase active site (A) – MALDI-TOF MS analysis of maturation of peptide 17C (B) and 17S (C) incubated 2 and 12 hours with anSMEcpe respectively

AnSMEcpe was incubated with each peptide (500 μM) under reducing conditions in the presence of AdoMet (1 mM).

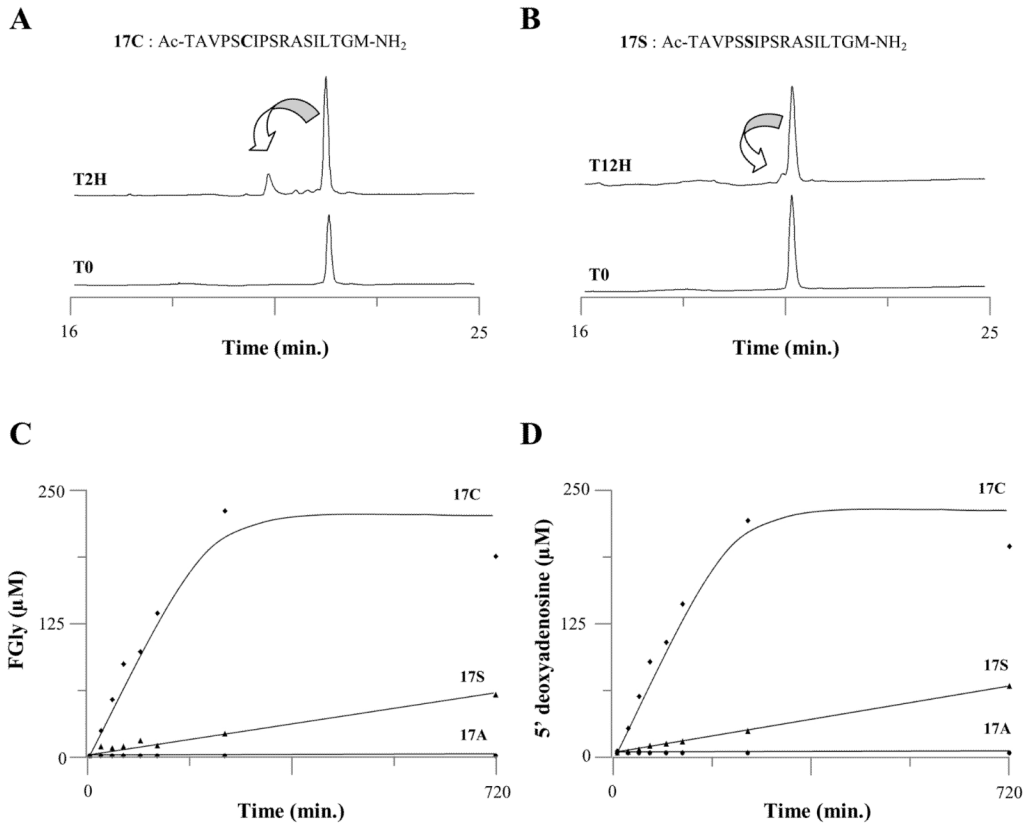

Figure 2. HPLC analysis of incubation reactions with peptide 17C (A) or 17S (B) and time-dependant formation of FGly-containing peptide (C) and 5′-deoxyadenosine (D) by anSMEcpe

AnSMEcpe was incubated with 17C (◆), 17S (▲) or 17A (●) peptide (500 μM) under reducing conditions in the presence of AdoMet (1 mM), DTT (6 mM) and dithionite (3 mM).

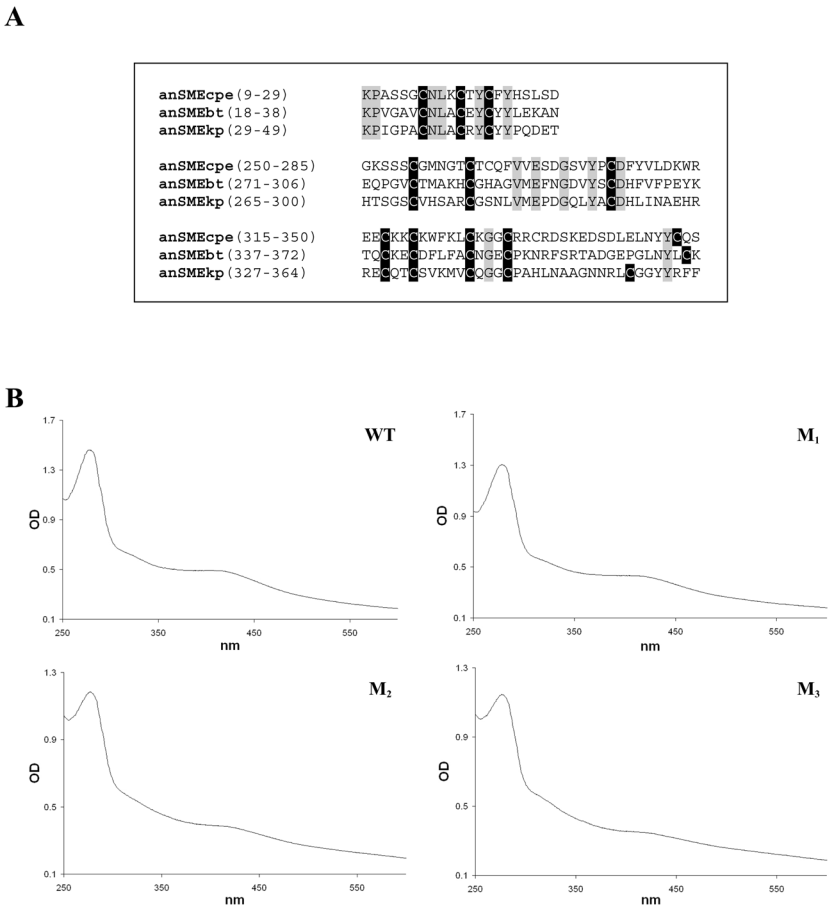

Figure 3. Sequence alignment of the three anSMEs putative clusters

(A) anSMEcpe (CPF_0616 from *Clostridium perfringens*), anSMEbt (BT_0238 from *Bacteroides thetaiotaomicron*) and anSMEkp (AtsB from *Klebsiella pneumoniae*). Sequence positions in the proteins are in brackets. The conserved cysteinyl residues are indicated in black boxes and the other conserved residues are shadowed **– UV visible absorption specta of reconstituted wild-type (WT) and M_1, M_2 and M_3 variants of anSMEbt (B)**.

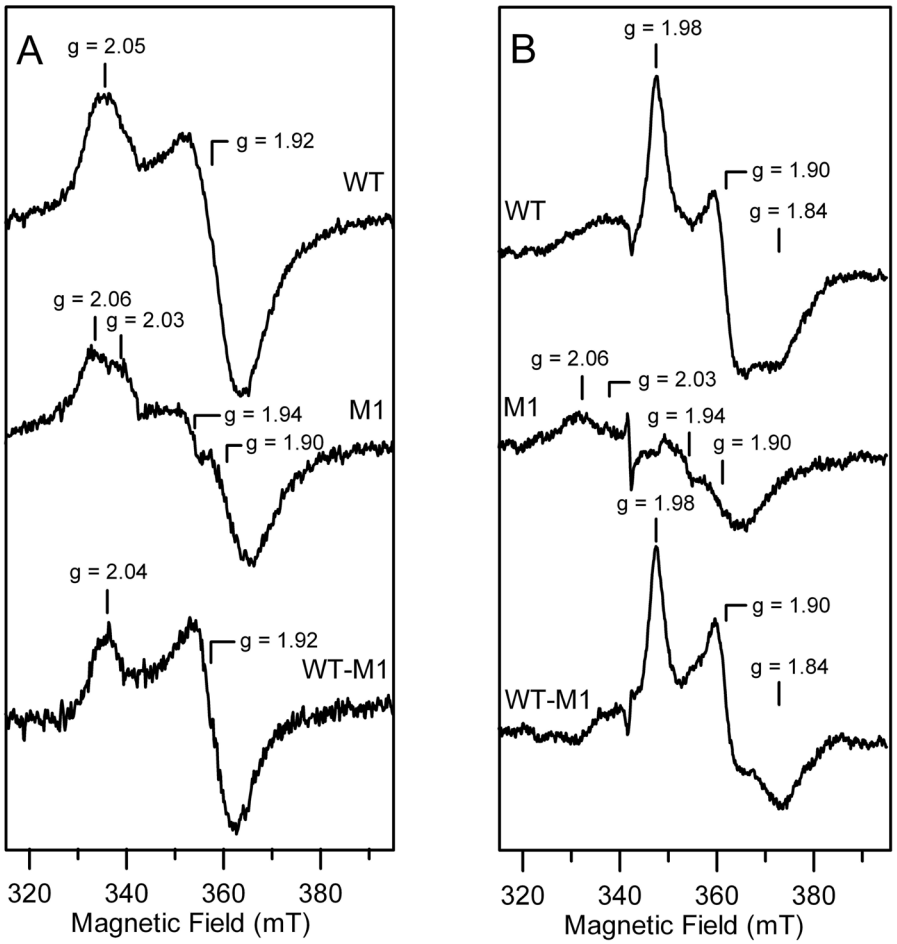

Figure 4. X-band EPR spectra of dithionite-reduced reconstituted samples of WT and M_1 mutant anSMEbt in the absence (A) and presence (B) of a 20-fold stoichiometric excess of AdoMet

The WT minus M_1 mutant difference spectrum at the bottom of each panel corresponds to the EPR spectrum of the $S = 1/2$ $[4Fe\text{-}4S]^+$ radical-AdoMet cluster with (B) and without (A) AdoMet bound at the unique Fe site. EPR spectra were recorded at 10 K with 20 mW microwave power, 0.65 mT modulation amplitude and a microwave frequency of 9.603 GHz. The spectrometer gain was 2-fold higher for the samples prepared without AdoMet. Samples of WT and M_1 mutant anSMEbt (each 0.4 mM) in Tris-HCl buffer, pH 7.5, were anaerobically reduced with a 10-fold stoichiometric excess of sodium dithionite.

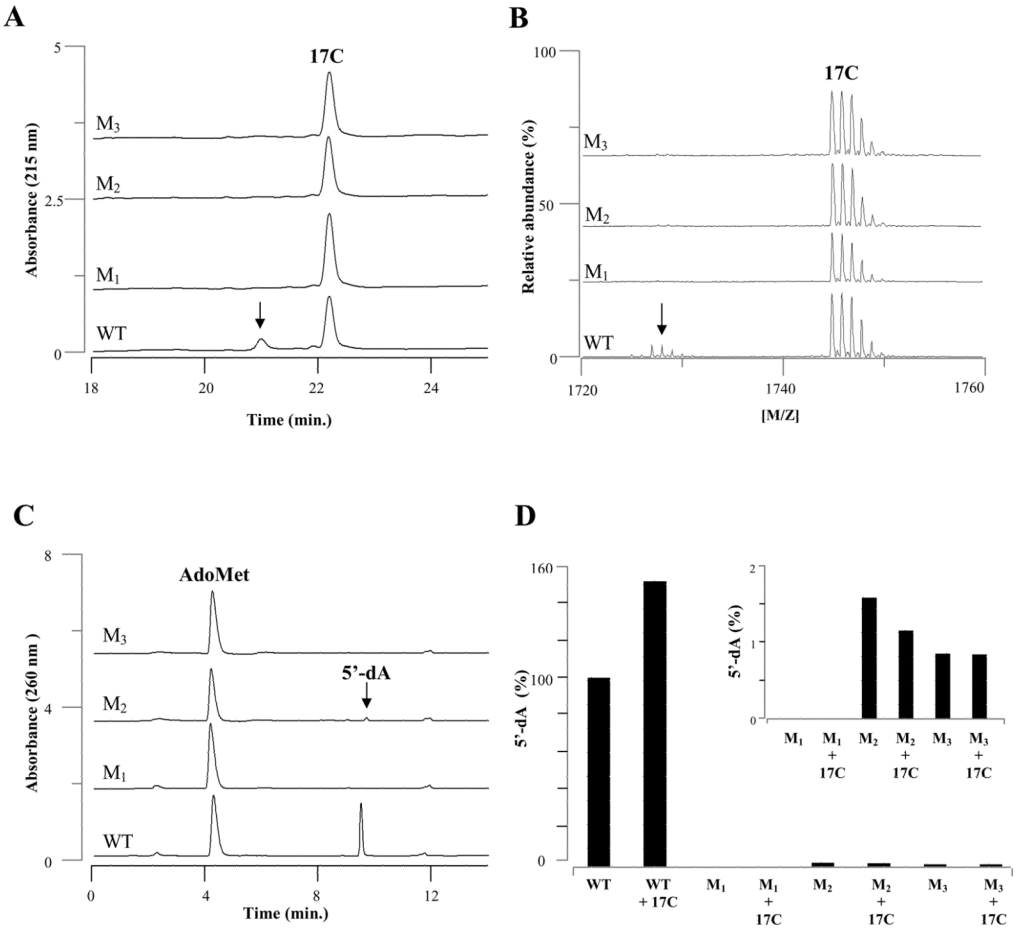

Figure 5. HPLC (A) and MALDI-TOF MS (B) analysis of the peptide maturation catalyzed by WT and M_1, M_2 and M_3 mutants of anSMEbt

The WT and mutant forms of anSMEbt (each 60 μM) were incubated with 17C peptide (500 μM) under reducing conditions in the presence of AdoMet (1 mM), DTT (6 mM) and dithionite (3 mM) for 4 hours under anaerobic and reducing conditions. (C) HPLC analysis of AdoMet cleavage catalyzed by WT or M_1, M_2 and M_3 mutants of anSMEbt in presence of 17C peptide. (D) Relative production of 5′-dA compared to the WT enzyme with or without substrate peptide (inset: magnified picture of the results obtained for the mutants).

Figure 6. Sequence alignment of anSMEcpe, QHNDH-AE, PqqE and the ST protein

Sequence positions in the proteins are in brackets. The percentage of similarity between the corresponding region of anSME and the different enzymes is indicated.

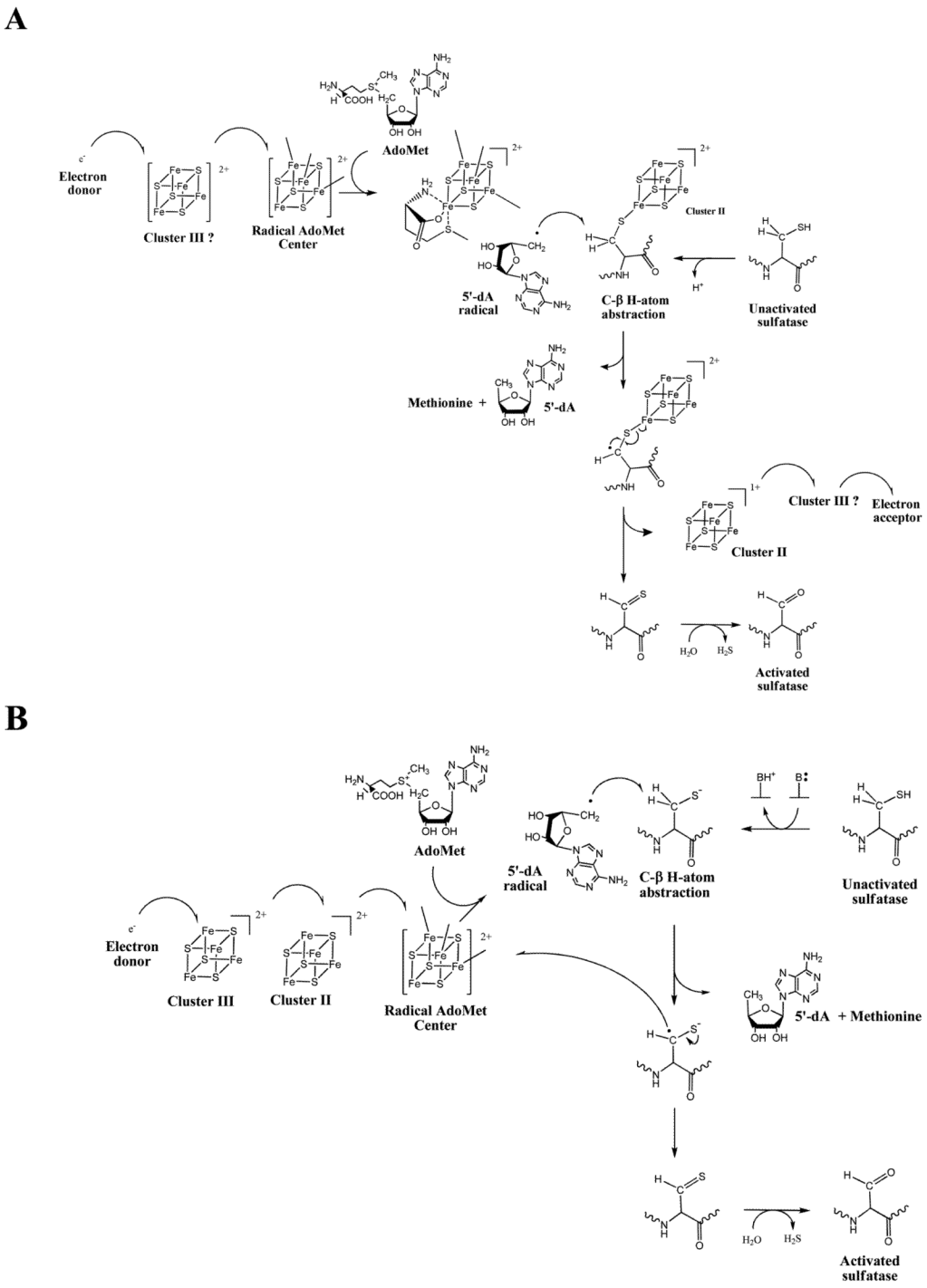

Figure 7. Two possible mechanisms for anSMEs with Cys-type sulfatases substrates

(A) After reduction of the radical AdoMet [4Fe-4S] center, AdoMet is reductively cleaved and the resulting 5′-deoxyadenosyl radical abstracts a Cβ hydrogen atom from cysteinyl residue of the substrate peptide that is ligated to a unique site of a [4Fe-4S] center (Cluster II). Cluster III is proposed to play a role in mediating electron transfer from the physiological electron to the radical AdoMet [4Fe-4S] cluster or from Cluster II to the physiological electron acceptor. (B) The peptidyl substrate is first deprotonated and AdoMet

is reductively cleaved. The resulting 5′-deoxyadenosyl radical abstracts a Cβ hydrogen atom from cysteinyl residue to generate a substrate radical that is converted to the thioaldehyde intermediate *via* outer-sphere electron transfer to the radical AdoMet cluster. In this scheme, the additional [4Fe-4S] centers, Clusters II and III, have a key role in mediating the initial electron transfer from the physiological electron to the radical AdoMet [4Fe-4S] cluster. In both mechanisms, a thioaldehyde intermediate is formed and further hydrolyzed to form the FGly residue with the release of hydrogen disulfide.